



Overview of the coordinated ground-based observations of Titan during the Huygens mission

Olivier Witasse,¹ Jean-Pierre Lebreton,¹ Michael K. Bird,² Robindro Dutta-Roy,² William M. Folkner,³ Robert A. Preston,³ Sami W. Asmar,³ Leonid I. Gurvits,⁴ Sergei V. Pogrebenko,⁴ Ian M. Avruch,⁴ Robert M. Campbell,⁴ Hayley E. Bignall,⁴ Michael A. Garrett,⁴ Huib Jan van Langevelde,⁴ Stephen M. Parsley,⁴ Cormac Reynolds,⁴ Arpad Szomoru,⁴ John E. Reynolds,⁵ Chris J. Phillips,⁵ Robert J. Sault,⁵ Anastasios K. Tzioumis,⁵ Frank Ghigo,⁶ Glen Langston,⁶ Walter Briskin,⁷ Jonathan D. Romney,⁷ Ari Mujunen,⁸ Jouko Ritakari,⁸ Steven J. Tingay,⁹ Richard G. Dodson,¹⁰ C. G. M. van't Klooster,¹¹ Thierry Blancquaert,¹¹ Athena Coustenis,¹² Eric Gendron,¹² Bruno Sicardy,¹² Mathieu Hirtzig,^{12,13} David Luz,^{12,14} Alberto Negro,^{12,14} Theodor Kostiuk,¹⁵ Timothy A. Livengood,^{16,15} Markus Hartung,¹⁷ Imke de Pater,¹⁸ Mate Ádámkóvics,¹⁸ Ralph D. Lorenz,¹⁹ Henry Roe,²⁰ Emily Schaller,²⁰ Michael Brown,²⁰ Antonin H. Bouchez,²¹ Chad A. Trujillo,²² Bonnie J. Buratti,³ Lise Caillault,²³ Thierry Magin,²³ Anne Bourdon,²³ and Christophe Laux²³

Received 17 November 2005; revised 29 March 2006; accepted 24 April 2006; published 27 July 2006.

[1] Coordinated ground-based observations of Titan were performed around or during the Huygens atmospheric probe mission at Titan on 14 January 2005, connecting the momentary in situ observations by the probe with the synoptic coverage provided by continuing ground-based programs. These observations consisted of three different categories: (1) radio telescope tracking of the Huygens signal at 2040 MHz, (2) observations of the atmosphere and surface of Titan, and (3) attempts to observe radiation emitted during the Huygens Probe entry into Titan's atmosphere. The Probe radio signal was successfully acquired by a network of terrestrial telescopes, recovering a vertical profile of wind speed in Titan's atmosphere from 140 km altitude down to the surface. Ground-based observations brought new information on atmosphere and surface properties of the largest Saturnian moon. No positive detection of phenomena associated with the Probe entry was reported. This paper reviews all these measurements and highlights the achieved results. The ground-based observations, both radio and optical, are of fundamental importance for the interpretation of results from the Huygens mission.

Citation: Witasse, O., et al. (2006), Overview of the coordinated ground-based observations of Titan during the Huygens mission, *J. Geophys. Res.*, *111*, E07S01, doi:10.1029/2005JE002640.

¹Research and Scientific Support Department, ESA, ESTEC, Noordwijk, Netherlands.

²Radioastronomisches Institut, Universität Bonn, Bonn, Germany.

³Jet Propulsion Laboratory, California Institute of Technology, Pasadena, California, USA.

⁴Joint Institute for VLBI in Europe, Dwingeloo, Netherlands.

⁵Australia Telescope National Facility, CSIRO, Epping, Australia.

⁶National Radio Astronomy Observatory, Green Bank, West Virginia, USA.

⁷National Radio Astronomy Observatory, Socorro, New Mexico, USA.

⁸Metsähovi Radio Observatory, Helsinki University of Technology, Kylmäla Finland.

⁹Swinburne University of Technology, Hawthorn, Australia.

¹⁰Observatorio Astronómico Nacional, Alcalá de Henares, Spain.

¹¹ESA, ESTEC, TEC Directorate, Noordwijk, Netherlands.

¹²LESIA, Observatoire de Paris-Meudon, France.

¹³Laboratoire de Planétologie et de Géodynamique, Nantes, France.

¹⁴Observatório Astronómico de Lisboa, Lisbon, Portugal.

¹⁵NASA Goddard Space Flight Center, Greenbelt, Maryland, USA.

¹⁶National Center for Earth and Space Science Education, Washington, D. C., USA.

¹⁷European Southern Observatory, Santiago, Chile.

¹⁸Department of Astronomy, University of California, Berkeley, California, USA.

¹⁹Lunar and Planetary Laboratory, University of Arizona, Tucson, Arizona, USA.

²⁰Division of Geological and Planetary Sciences, California Institute of Technology, Pasadena, California, USA.

²¹Caltech Optical Observatories, California Institute of Technology, Pasadena, California, USA.

²²Gemini Observatory, Hilo, Hawaii, USA.

²³Laboratoire EM2C, Ecole Centrale Paris, CNRS-UPR288, Châtenay-Malabry, France.

1. Introduction

[2] In 2003, the International Astronomical Union Commission 16 (Physical Study of Planets and Satellites) “endorsed astronomical observations of the Saturnian system at the time of the NASA and ESA Cassini/Huygens mission to the Saturnian system. The attention of the world-wide astronomical community is drawn to the unique scientific opportunities presented by the presence of a long-lived orbiting spacecraft in the Saturnian system and a Titan Probe. Observations of all types, ground- and space-based, are encouraged during the course of the mission (nominally 2003–2008), including observations of Saturn, the rings, Titan, and the icy satellites.” It was therefore decided to support and coordinate, at the level of the Huygens Project Scientist Team, a series of ground-based observations at the time of the Huygens mission. The results from the observing campaign are presented in this special section.

[3] The Huygens mission was carried out successfully on 14 January 2005. An overview of the mission is given by *Lebreton et al.* [2005], while the first scientific results from all experiments are reported by *Bird et al.* [2005], *Fulchignoni et al.* [2005], *Israel et al.* [2005], *Niemann et al.* [2005], *Tomasko et al.* [2005], and *Zarnecki et al.* [2005].

[4] At the time of the mission, no fewer than 17 radio telescopes were pointed at Titan and tuned to the frequency of the Huygens “channel A” carrier signal at 2040 MHz. [*Lebreton et al.*, 2005]. An Earth-based radio-tracking effort on this scale was not planned during the original design of the mission and required major coordination that included dry-run observations in August and November 2004. The Huygens radio astronomy ground-based segment was designed to achieve the following three goals: real-time detection of the Huygens carrier signal; Doppler tracking as an enhancement to the Doppler Wind Experiment (DWE) [*Folkner et al.*, 2006]; acquisition of Very Long Base Interferometry (VLBI) data for determining the position of the Probe in the celestial plane.

[5] Eight large optical observatories participated in coordinated observations of Titan before, during and after the Huygens mission. The first objective was to carry out scientific observations of Titan in various fields: near-infrared studies of the atmosphere and of the surface [*de Pater et al.*, 2006; *Hartung et al.*, 2006; *M. Hirtzig et al.*, Atmospheric and surface features as observed with NAOS/CONICA at the time of the Huygens’ landing, submitted to *Journal of Geophysical Research*, 2006 (hereinafter referred to as *Hirtzig et al.*, submitted manuscript, 2006); *A. Negrao et al.*, Two-micron spectroscopy of Huygens’ landing site on Titan with VLT/NACO, submitted to *Journal of Geophysical Research*, 2006 (hereinafter referred to as *Negrao et al.*, submitted manuscript, 2006)], determination of the zonal wind [*Luz et al.*, 2006; *Kostiuk et al.*, 2006]; stratospheric haze distribution [*Adámkovicš et al.*, 2006; *de Pater et al.*, 2006], ethane vertical profile determination (*T. A. Livengood et al.*, High-resolution infrared spectroscopy of ethane in Titan’s atmosphere in the Huygens epoch, *Journal of Geophysical Research*, 2006; hereinafter referred to as *Livengood et al.*, submitted manuscript, 2006) and global imaging. The second objective was to detect the Probe’s entry into Titan’s atmosphere [*Lorenz et al.*, 2006; *de Pater et al.*, 2006].

[6] All these observations in various domains of the electromagnetic spectrum were complementary to the Huygens measurements. The radio astronomy segment proved especially valuable following the loss of the Cassini channel A receiver in that it largely recovered the primary goal of the Doppler Wind Experiment [*Bird et al.*, 2005; *Lebreton et al.*, 2005; *Folkner et al.*, 2006]. Other astronomical observations provided key information on the atmosphere and surface properties. Section 2 gives an overview of the coordinated set of observations, and section 3 outlines the scientific results achieved so far. Engineering achievements are summarized in section 4.

2. Overview of the Ground-Based Observations

[7] Many observations of Titan were made during the Huygens mission. Here, only the coordinated ground-based observations are briefly described and put into context.

2.1. Radio Tracking of the Huygens Signal

[8] Seventeen radio telescopes listed in Table 1 and displayed in Figure 1 participated in the monitoring of the carrier signal driven by the DWE ultra-stable oscillator onboard the Huygens Probe and formed the radio astronomy segment of the mission. This segment consisted of two types of observations:

[9] 1. All 17 radio telescopes participated in Very Long Base Interferometry (VLBI) observations of the Huygens Probe. Of these, 15 telescopes were tuned to the Huygens channel A carrier frequency of 2040 MHz, while two others did not observe the Probe at this frequency but were involved in the overall “phasing-up” the network of radio telescopes by observing the calibrator sources at frequencies not covering the value of 2040 MHz. The goal of the VLBI observations, led by the Joint Institute for VLBI in Europe (JIVE), was to reconstruct the projection of the descent trajectory on the plane of the sky, with an expected linear accuracy of the order of 1 km.

[10] 2. Six radio telescopes from the entire network of seventeen participated in Doppler observations of the Huygens Probe, in parallel with the VLBI observations. The goal of these observations, led by NASA’s Jet Propulsion Laboratory, was to generate a full two-dimensional characterization of Titan’s horizontal wind field during the Probe’s descent from a combination of the planned Doppler measurements on the Probe-Orbiter and Probe-Earth radio links. The two largest radio telescopes of the network, the NRAO R.C. Byrd Green Bank and CSIRO Parkes telescopes were equipped with NASA Deep Space Network Radio Science Receivers. These devices were able to digitally record the Huygens’ carrier radio signals and detect them in real-time. Four additional telescopes of the Very Long Baseline Array (VLBA), NRAO Pie Town, Kitt Peak, Owens Valley and Mauna Kea, were equipped with JPL-built PC-based Digital Doppler Recorders.

[11] Both parts of the radio astronomy segment of the Huygens mission have been built on the heritage of previous similar experiments. In particular, the Huygens Doppler tracking experiment with Earth-based radio telescopes evolved from the JPL-led observations of the Galileo mission in the atmosphere of Jupiter [*Folkner et al.*, 1997a] and earlier observations of Pioneer Venus probes

Table 1. Radio Telescopes Involved in the Radio Astronomy Segment of the Huygens Mission^a

	Radio Telescope	Institute, Country	Diameter, m	Observing Time (ERT/UTC)	
				Start	Stop
1.	Green Bank ^b	NRAO, USA	100	09:31:10	12:15:00
2.	VLBA North Liberty	NRAO, USA	25	09:31:10	13:15:00
3.	VLBA Fort Davis	NRAO, USA	25	09:31:10	13:45:00
4.	VLBA Los Alamos	NRAO, USA	25	09:31:10	14:00:00
5.	VLBA Pie Town	NRAO, USA	25	09:31:10	14:15:04
6.	VLBA Kitt Peak	NRAO, USA	25	09:31:10	14:15:00
7.	VLBA Owens Valley	NRAO, USA	25	09:30:09	14:49:14
8.	VLBA Brewster	NRAO, USA	25	09:31:10	14:48:00
9.	VLBA Mauna Kea	NRAO, USA	25	09:31:10	16:00:00
10.	Kashima	NIICT, Japan	34	09:31:10	16:00:00
11.	Sheshan (Shanghai)	NAOC & ShAO, China	25	10:01:10	16:00:00
12.	ATCA ^c	Australia	5 × 22	10:01:10	16:00:00
13.	Nanshan(Urumqi) ^c	NAOC, China	25	11:31:10	16:00:00
14.	Mopra	ATNF, Australia	22	10:10:10	16:00:00
15.	Parkes ^b	ATNF, Australia	64	12:26:23	16:00:00
16.	Hobart	U Tasmania, Australia	26	11:13:10	16:00:00
17.	Ceduna	U Tasmania Australia	30	10:13:10	16:00:00

^aERT/UTC, Earth Received Time in the UTC scale.

^bProvided real-time detection of the Huygens channel A carrier signal at 2040 MHz.

^cUsed as phase referencing anchors, but did not observe the carrier signal.

[Counselman *et al.*, 1979]. VLBI tracking of planetary spacecraft for navigation was developed in the mid-1970s and has been frequently used since then [Thornton and Border, 2003]. VLBI observations of planetary probes have also been used to measure lunar rotational dynamics [King *et al.*, 1976; Slade *et al.*, 1977] and winds on Venus [Counselman *et al.*, 1979; Preston *et al.*, 1986; Sagdeyev *et al.*, 1992]. We note that the VLBI technique offers extremely high angular resolution that is inversely proportional to the baseline (distance) between the telescopes involved. At wavelengths of radio domain and baselines of up to 10,000 km, the VLBI technique enables a milliarc-second-scale “sharpness” in determination of the position of a point-like source of emission. Recent improvements in the VLBI technique, including wider recording bandwidths and phase-referencing, were employed for the Huygens observations, providing much greater sensitivity than previous VLBI observations of space probes.

2.2. Observations of Titan

[12] The following telescopes (listed in Table 2) observed Titan with various scientific objectives:

[13] 1. The National Astronomical Observatory of Japan Subaru telescope (Hawaii) was equipped with the NASA Goddard Space Flight Center Heterodyne Instrument for Planetary Wind And Composition, HIPWAC [Kostiuk *et al.*, 2001, 2005]. The goal was to directly measure the magnitude and direction of Titan’s stratospheric zonal wind by measurement of the Doppler-shift of ethane lines near 12 μm emitted from Titan’s stratosphere. Observations were scheduled on 13, 14, and 15 January. Poor weather prevented measurements on 13 January, permitted only limited measurements on 14 January, but allowed better results on 15 January.

[14] 2. The UV-Visual Echelle Spectrograph (UVES) on the Very Large Telescope (VLT) was used to measure the Doppler-shifted solar spectrum reflected by the Titan’s atmosphere in the visible range [Luz *et al.*, 2006]. Zonal winds in the stratosphere are inferred from such an observation. Titan was not visible with the VLT at the time of the

Huygens mission. 32 exposures spanned over 4 nights were performed around 14 January 2005.

[15] Three telescopes were used to study the atmosphere and surface of Titan in the near-infrared (all using adaptive optics), by virtue of the weak methane absorption found at certain wavelengths and allowing to probe down to the surface.

[16] 1. The VLT Yepun telescope observed Titan on 15 and 16 January by means of the NAOS/CONICA (NACO) instrument. Several modes of NACO were used: (1) narrow-band filter imaging, gathering information around 1.3 and 2 micron; (2) spectroscopy from 2.0–2.5 micron; (3) Simultaneous Differential Imager (SDI) near 1.6 micron; and (4) Fabry-Perot imaging in the K-band (2.00–2.18 microns).

[17] 2. Observations with the Near-Infrared Camera (NIRC2) camera at the KECK II were scheduled on 14, 15, 16, and 17 January. The camera was used in high angular resolution mode. Several filters were used between 1.485 and 2.299 μm .

[18] 3. The William Herschel Telescope equipped with the NAOMI/OASIS system observed on 10, 19, and 22 January, in the range 0.8 to 1 microns.

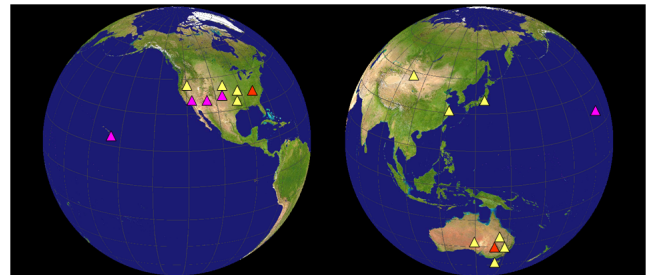


Figure 1. Approximate locations of Earth-based radio telescopes involved in the radio astronomy segment of the Huygens mission. All seventeen telescopes participated in VLBI observations. Two telescopes shown in red (Green Bank and Parkes) participated in real-time detection of the Huygens Channel A carrier signal at 2040 MHz. The latter two plus four VLBA telescopes shown in purple participated in Doppler measurements.

Table 2. Optical Astronomical Observatories^a

Facility/Instrument	Wavelength	Time of Observation	Goal: Attempt to Detect the Probe Entry	Goal: Titan Science
Subaru/HIPWAC	12 μm	13, 14, 15 January	no	zonal wind measurements, ethane profile
VLT/UVES	420–620 nm	7, 12, 14, 15 January	no	zonal wind measurements
VLT/NACO	1.2–2.5 μm range	18–19 December [2004]; 15, 16 January	no	atmosphere and surface characterization
VLT/SINFONI	1.45–2.45 μm range	28 February	no	atmosphere and surface characterization
Keck/NIRC2	several filters between 1.485 and 2.299 μm	14, 15, 16, 17 January	yes	atmosphere and surface characterization
WHT/NAOMI-OASIS	0.8–1 μm range	10, 19, 22 January	no	atmosphere and surface characterization
IRTF/TEXES	near-IR	14 January	yes	atmosphere characterization
HALE	IR and visible	canceled (bad weather)	yes	
GEMINI	Near-IR	canceled (bad weather)	yes	
Observatoire du Pic du Midi	1.28 μm	9–17 January	no	effects on Titan's surface of the Saturn's opposition
14-inch telescope at New Mexico Skies Observatory	visible	observations since 2003, including the night of the Huygens mission	no	monitoring of cloud activity
HST/STIS	visible	canceled	yes	
Stellar occultation campaign	IR and visible	November 2003	no	atmosphere characterization

^aColumn 4 indicates if the planned observation was related to the detection of the Huygens Probe entry (yes or no). Scientific goals related to Titan are given in column 5. Subaru is the National Astronomical Observatory of Japan 8.2-m telescope, located at Mauna Kea (Hawaii). HIPWAC is the NASA Goddard Space Flight Center Heterodyne Instrument for Planetary Wind And Composition. VLT is the European Southern Observatory 8-m Very Large Telescope, located in Chile. UVES is the UV-Visible Echelle Spectrograph mounted on one of the VLT telescope. NACO is an adaptive optics system mounted on the Yepun VLT telescope. SINFONI is the new adaptive optics assisted integral-field spectrometer mounted on the Yepun VLT unit. Keck is a 10-m telescope located at the summit of Mauna Kea (Hawaii), operated as a scientific partnership among the California Institute of Technology, the University of California, and the National Aeronautics and Space Administration. The NIRC2 is an adaptive optics system mounted on the Keck telescope. WHT is the William Herschel Telescope, 4.2 m telescope, located in La Palma (the Canary Islands). OASIS is an adaptive optics system operating first at the CFHT (Hawaii) with PUEO and then at the WHT with NAOMI. IRTF is the NASA Infrared Telescope Facility. IRTF is a 3-m telescope located at the summit of Mauna Kea (Hawaii). TEXES is a high-resolution grating spectrograph mounted on IRTF. HALE is the Palomar 5.1-m telescope, located in north San Diego, California. Gemini is an 8-m optical/infrared telescope located in Hawaii. The Pic du Midi Observatory is located in the French Pyrenees Mountains. 1- and 2-m telescopes are being used for professional reasons. HST is the Hubble Space Telescope, and STIS is the Space Telescope Imaging Spectrograph.

[19] Two additional observations deserve to be mentioned, even if they were not formally part of the coordinated ground-based observations during the Huygens mission:

[20] 1. The Pic du Midi (France) telescope was observing the surface of Titan. The interest was the study of the effect of Saturn's opposition (13 January 2005) on the surface. The observation was carried out in the infrared at 1.28 micron.

[21] 2. A simple whole-disk cloud monitoring program was developed using a 14-inch telescope located at New Mexico Skies Observatory. Observations were performed in

2003, 2004 and 2005, including the time of the Huygens mission.

[22] Three articles of this special section deal with observations performed outside the "Huygens mission window": *Ádámkovics et al.* [2006] present observations conducted on 28 February 2005 with the new adaptive optics assisted integral-field spectrometer SINFONI mounted on the VLT. *Hartung et al.* [2006] describe an experiment aiming to map solid CO₂ ice on the surface, based on data obtained with NACO/VLT on 18 and 19 December 2004. B. Sicardy et al. (The two Titan stellar occultations of 14 November 2003, submitted to *Journal of Geophysical Research*, 2006; here-

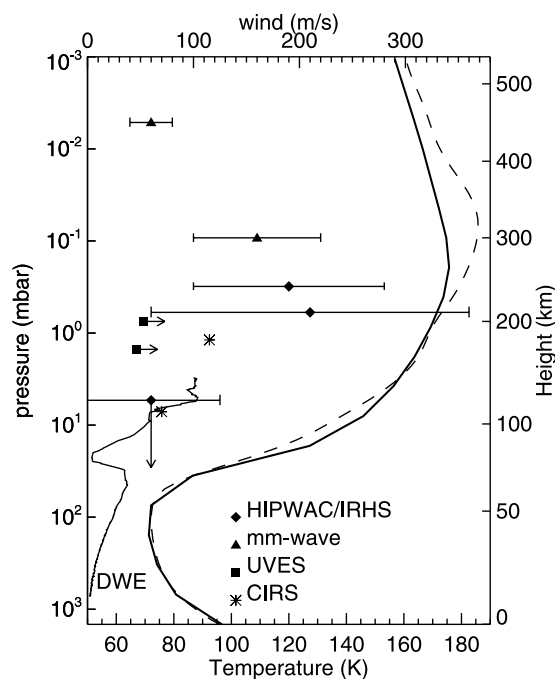


Figure 2. Velocity retrievals in Titan's atmosphere [from Kostiuk *et al.*, 2006]: HIPWAC/IRHS [Kostiuk *et al.*, 2006]; UVES [Luz *et al.*, 2006]; DWE [Bird *et al.*, 2005]; mm-wave [Moreno *et al.*, 2005]; and CIRS [Flasar *et al.*, 2005]. Different altitudes are probed by the different techniques. Results indicate large wind variation with height and possibly with time. The Cassini CIRS retrieved velocities plotted have been adjusted to account for ~ 55 m/s wind at 10 mbar measured by the Doppler Wind Experiment. The pre-Cassini [Yelle *et al.*, 1997] (solid line) and Cassini CIRS (dashed line) thermal profiles are shown.

inafter referred to as Sicardy *et al.*, submitted manuscript, 2006) report on the two Titan stellar occultations campaign of November 2003. This observation provided important constraints on the validation of the upper atmosphere model of Titan prior to the Huygens release.

2.3. Attempt to Detect the Probe Entry

[23] Five telescopes (see column 4 of Table 2) were devoted to the detection of the emission formed during the Huygens Probe's entry into Titan's atmosphere and due to dissipation of kinetic energy. Details are given by Lorenz *et al.* [2006]. The planned observations included (1) the NIRC2 camera mounted on the KECK II telescope (Hawaii); (2) the TEXES high-resolution spectrometer on IRTF (Hawaii); (3) the Near InfraRed Imager on the Gemini telescope (Hawaii); (4) the Palomar Double Spectrograph on the Hale telescope (California); and (5) the Space Telescope Imaging Spectrograph (STIS) on board the HST.

3. What do These Observations Bring to Our Understanding of Titan?

3.1. Stratospheric Temperatures

[24] Sicardy *et al.* (submitted manuscript, 2006) derived temperature profiles between 400 and 600 km height (see their Figure 9). The most interesting feature is a sharp

inversion layer near the 515 ± 5 km altitude level. At that level, the temperature locally increases by 15 K in only 6 km, and the peak value of the gradient dT/dz reaches values as high as +6 K/km. This layer has also been observed by the HASI experiment aboard Huygens, at around 507 ± 15 km. Further work is needed to understand the difference in altitude.

3.2. Zonal Winds

[25] The direct Doppler wind observations on Subaru [Kostiuk *et al.*, 2006] and VLT [Luz *et al.*, 2006] are combined with other direct ground-based measurements and measurements from Cassini DWE to retrieve a first altitude profile for zonal winds on Titan from ~ 10 to ~ 450 km altitude (Figure 2). A prograde wind is retrieved throughout and significant increase in wind velocity is seen in the upper stratosphere. Wind speeds deduced from stellar occultations (e.g., Sicardy *et al.*, submitted manuscript, 2006) and from thermal maps by CIRS [Flasar *et al.*, 2005] are in good agreement with the Doppler retrievals. Current dynamical models qualitatively agree with this profile and can be further constrained and improved using the wind altitude profile. Observational and theoretical model results lead to a better understanding of atmospheric dynamics of slowly rotating bodies. Evidence of temporal and possibly spatial variability as well as the possible probe of Titan's mesosphere by HIPWAC provide new directions for further studies from Cassini as well as from ground-based observatories.

[26] An improved wind profile for the middle and stratosphere and below with higher temporal resolution (2–3 seconds) than that presented in the preliminary analysis of Bird *et al.* [2005] is published in this special section [Folkner *et al.*, 2006], with a first high vertical resolution display and interpretation of the winds near the surface and planetary boundary layer. The main features are (1) the drop in wind speed to near zero at an altitude between 65 and 75 km; (2) the slow and retrograde wind speed between 1 and 5 km altitude, reversing to slightly prograde at the surface; and (3) the ~ 1 m/s eastward surface wind consistent with the theoretical prediction of a surface gradient-wind less than 2 m/s.

[27] Zonal wind profiles are deduced at about 250 km altitude from stellar occultation measurements (Sicardy *et al.*, submitted manuscript, 2006). A strong asymmetry between the northern and southern hemispheres has been found in terms of wind intensity (see Figure 3): about 215 m/s at 55N, 150 m/s at the equator, and then zero in the summer (southern) hemisphere.

3.3. Atmospheric Density and Composition

[28] (Sicardy *et al.*, submitted manuscript, 2006, Figure 8) report on stratospheric density profiles. There is a good agreement between the retrieved profiles and Yelle's engineering model predictions in the 400–500 km altitude range [Yelle *et al.*, 1997]. However, a closer inspection shows that the density profiles are about 35% denser (at a given altitude) than Yelle's profile (or about 15 km higher, for a given density). Considering the uncertainty domain, this discrepancy remains nevertheless marginal.

[29] The vertical distribution of ethane is discussed by Livengood *et al.* (submitted manuscript, 2006), based on

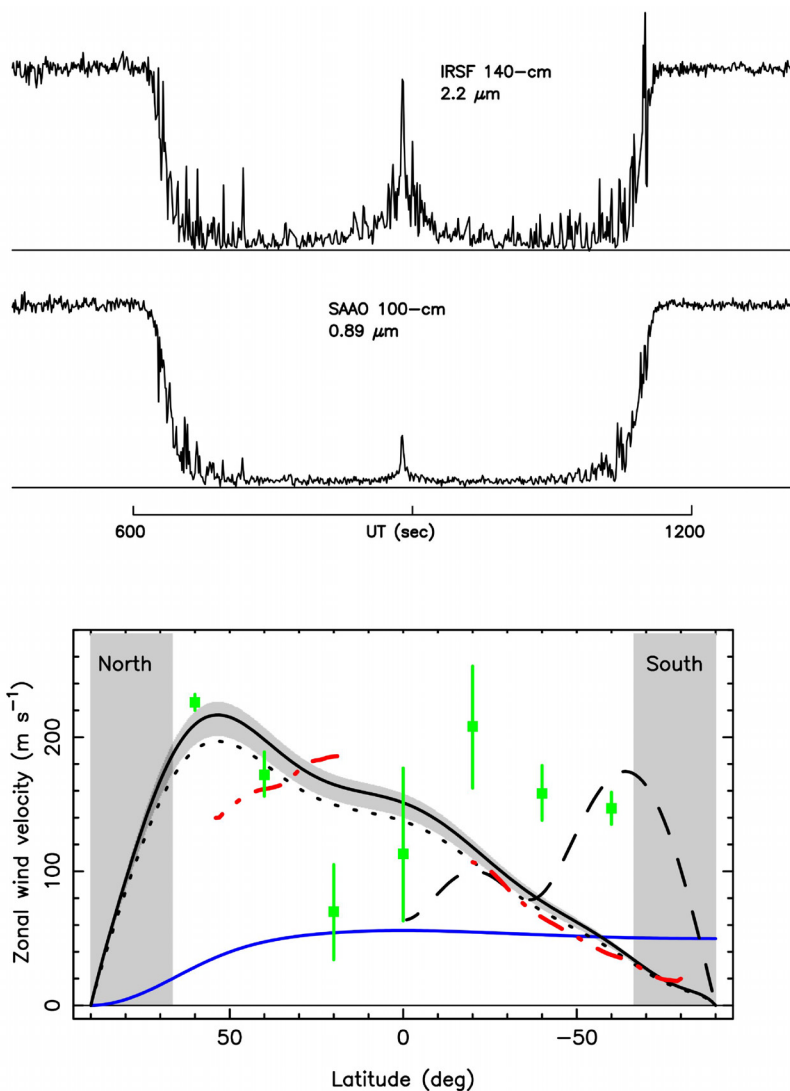


Figure 3. (top) Two occultation light curves observed on 14 November 2003 from the same site at Sutherland (South Africa), in two different bands: 0.89 microns at the South Africa Astronomical Observatory (SAAO) and 2.2 microns at the InfraRed Survey Facility of Nagoya University (IRSF). The differences in the central flashes are solely due to the differential extinctions of the hazes, which become more and more transparent at longer IR wavelengths. (bottom) Zonal wind profile derived from the November 2003 central flash analysis (solid black curve), compared to the Cassini-CIRS profile (red dash-dots) obtained one year later. The wind profile is also compared with other profiles obtained in the previous years (Sicardy et al., submitted manuscript, 2006).

high-resolution infrared spectroscopy performed with the Subaru telescope and the HIPWAC instrument. The observed morphology of the C_2H_6 spectroscopic signature differs significantly from earlier observations. The spectroscopy favors a vertical distribution of C_2H_6 that is enhanced in the mesosphere. An ethane mole fraction of 9.4 ± 2.0 to 10.8 ± 2.4 parts per million by volume (ppmv) is retrieved for the stratosphere, depending on which of two acceptable mole fraction profiles is assumed. These concentrations are consistent with earlier retrievals from IR heterodyne spectroscopy. An enhanced mole fraction in the mesosphere of 120 ± 30 ppmv is found with a profile that assumes differing vertically uniform concentrations in the stratosphere and mesosphere. The other acceptable profile,

which has a steady gradient through the mesosphere, reaches a similar concentration at about 440 km above the stratopause.

3.4. Cloud Activity

[30] The Keck II captured Titan some moments after the Huygens Probe reached its target (Figure 4). No clouds were detected on that day. A feeble cloud appeared on 15 January and remained visible through 17 January. The bright large southern pole feature observed in Titan's atmosphere since 1999 and until recently with adaptive optics is not evident either in the VLT/NACO data on 15 or 16 January. The brightness observed at the location where it usually appears (at 2.12 micron anyway) is about

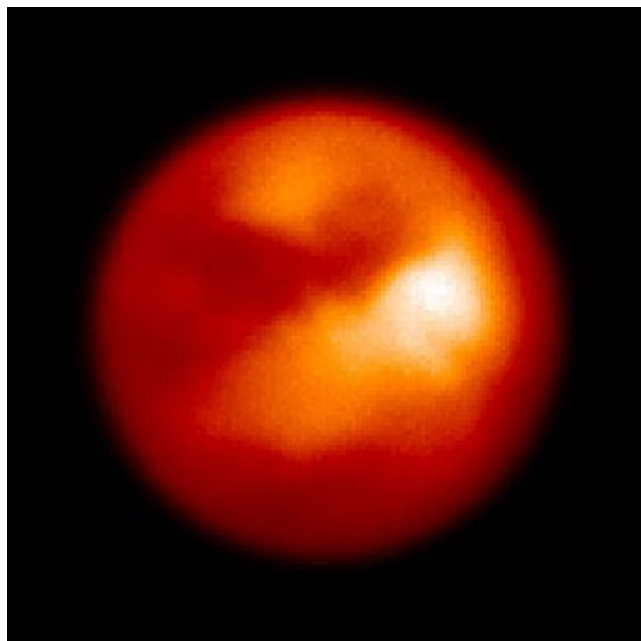


Figure 4. Keck image. Near-infrared surface image of Titan captured with Keck adaptive optics system moments after the Huygens Probe reached its target. The bright and dark patterns on Titan's surface may be regions of solid ice and of liquid hydrocarbons.

10% brighter with respect to the rest of the limb, and since this is our intrinsic error bar here for the Fabry-Perot Interferometer, Hirtzig et al. (submitted manuscript, 2006) cannot claim a detection. The regular Narrow-Band filters do not see any hint for such a feeble phenomenon, confirming the lack of cloud activity above the South Pole of Titan. On the other hand, the NACO images clearly show at several wavelengths (in the 2.12–2.15 micron range) a feature near the south pole but at higher latitudes (60–70°S) on the Western lower side; this feature was reported by Hirtzig et al. [2006] as a companion to the main southern cloud or vortex. At the time of the Huygens descent it presents a contrast of 87% with respect to the surrounding areas.

[31] This lack of south polar cloud activity on 14 January 2005 is confirmed by the 14 inch telescope photometry project and Gemini observations [Schaller et al., 2005]. No cloud activity at the Huygens landing site near the equator has ever been observed in adaptive optics images during the past four years of observations. South polar clouds were observed in nearly all adaptive optics images from October 2001 until November of 2004 when south polar cloud activity dramatically decreased until at least April 2005 (E. L. Schaller et al., Dissipation of Titan's south polar clouds, submitted to *Icarus*, 2006). This decrease in south polar cloud activity occurred following an extremely large cloud event in October of 2004, where the south polar clouds brightened to over fifteen times their typical values [Schaller et al., 2006]. The Huygens landing occurred during a quiescent period of cloud activity on Titan which lasted for at least five months. The lack of south polar cloud activity observed during this time period may be the

beginning of seasonal change and/or could be related to the large cloud event of October 2004.

3.5. Haze Distribution

[32] The tropospheric haze enhancement near the South Pole is confined to latitudes above 40S, and aerosol extinction there is retrieved to be enhanced by a factor of 1.7 relative to the latitude of the Huygens landing site [Ádámkóvics et al., 2006]. The stratospheric extinction is measured to increase linearly at a rate of $0.65 \pm 0.05\%$ per degree latitude from 40S into the Northern mid latitudes. Both of these values have been determined in the context of the Huygens/DISR measurement that demonstrate a constant tropospheric haze extinction. The observations presented here reveal that the tropospheric haze enhancement observed in 2001, shortly before the summer solstice at the South Pole (in October 2002), has thinned and is far less prominent than in 2005. However, the interpretation by Ádámkóvics et al. [2004] of an enhancement specifically near the altitude of the tropopause must be revised in light of the Huygens/DISR measurements, and further observations are necessary to show if indeed there is a preferential altitude in the troposphere at which the extinction enhancement occurs. The redistribution of tropospheric haze is a new example of large-scale aerosol dynamics, like the seasonal stratospheric haze asymmetry that has been observed, for example, from the Hubble Space Telescope [Lorenz et al., 2004] and from the ground [Gibbard et al., 2004].

3.6. Surface

[33] The dark/bright surface contrast analysis at different wavelengths indicated perhaps the presence of coarser grained frost in the dark areas compared to the bright regions, and/or the presence of additional absorbers in these dark areas, such as NH_3 and/or NH_4SH frost [de Pater et al., 2006; Hirtzig et al., submitted manuscript, 2006].

[34] Surface albedo maps were produced at 2 wavelengths [Ádámkóvics et al., 2006, Figure 12], giving complementary information on the bright spot detected by the Cassini/VIMS experiment. Bright spots detected by the Very Large Telescope show a spectral response compatible with methane and water ices (Hirtzig et al., submitted manuscript, 2006). Surface albedo of the Huygens landing site was estimated to be 0.12 at 2.03 microns and 0.02 at 2.12 microns, very close to the values calculated for dark areas (Negrao et al., submitted manuscript, 2006).

[35] CO_2 ice was not detected at the surface [Hartung et al., 2006; Hirtzig et al., submitted manuscript, 2006]. At subearth longitudes 284°W and 307°W , it was found that a partial coverage of CO_2 ice does not exceed 7% or 14% for bright and dark surface regions, respectively. At 65 mas angular resolution, the PSF sampled a surface region of 1260 thousand km^2 . The percentages translate into a maximum area of 90 or 180 thousand km^2 filled with solid CO_2 ice. The enigmatic bright 5 micron spot at 80°W , 25°S described by Barnes et al. [2005] is not covered by the longitude range of these observations, but would be easily detectable if it were pure solid CO_2 ice [Hartung et al., 2006]. The Huygens landing site was specifically observed by the Very Large Telescope (Figure 5). This gives a broader context to the probe measurements (Hirtzig et al., submitted manu-

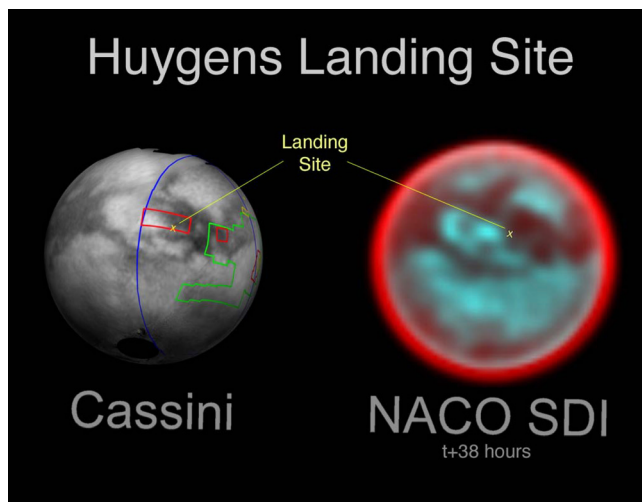


Figure 5. Comparison between the NACO/SDI image and an image taken by Cassini/ISS, showing the high consistency between both measurements. The Cassini image shows the Huygens landing site map wrapped around Titan, rotated to the same position as the January NACO SDI observations. The Cassini/ISS image is courtesy of NASA, JPL, Space Science Institute. The colored lines delineate the regions that were imaged by Cassini at differing resolutions. The lower-resolution imaging sequences are outlined in blue. Other areas have been specifically targeted for moderate- and high-resolution mosaicking of surface features. These include the site where the Huygens Probe has touched down on 14 January 2005 (marked with the yellow x (latitude 10.3°S ; longitude 167.7°E), part of the bright region named Xanadu (easternmost extent of the area covered), and a boundary between dark and bright regions. Image and text are part of a press release from ESO (24 February 2005). The red color corresponds to an atmospheric filter at 1.625 micron, while the blue color corresponds to a filter for the surface at 1.600 and 1.575 micron.

script, 2006; Negrao et al., submitted manuscript, 2006). The data indicate a high gradient of luminosity in this area.

4. Engineering/Science Support Achievements

4.1. Support in the Determination of the Huygens Trajectory and Attitude

[36] Data from the VLBI and Doppler ground-based radio observations of the probe are the key to the determination of the probe trajectory and other dynamical characteristics. Measurements of both the Probe plane of sky motions, from the VLBI data, and the Probe-Earth relative velocities, from the Doppler observations, are being used. The VLBI data analysis indicates that the probe trajectory in the plane of the sky will be determined to an accuracy of about 1 km [Pogrebenko et al., 2004]. The radio data set will also provide in the near future additional pieces of information:

[37] 1. Measurements of the carrier signal frequency are being used to constrain some attitude parameters of the Huygens Probe during its descent, namely the Probe pendulum motion and spin. These parameters are needed for a careful analysis of the scientific payload data set.

[38] 2. Titan astrometry (measurements of the celestial position and parameters of the motion of the planet).

[39] Folkner et al. [2006] determined the landing position to be latitude 10.33°S , longitude 192.32°W (167.68°E), based on the landed Doppler data combined with the integrated descent trajectory, in excellent agreement with the initial values published by Lebreton et al. [2005].

4.2. Real-Time Detection of the Huygens Probe's Signal

[40] On 14 January 2005, the NRAO R.C. Byrd Green Bank Telescope directly detected the Huygens carrier signal at around 10:19:26 Earth Received Time UTC, thus providing invaluable confirmation of the overall state of the mission some 6 hours before telemetry data could reach the Earth via the Cassini relay. The detection indicated that (1) the Probe entry had been successful, (2) the pilot chute had been deployed and the back cover had been ejected, (3) the main parachute had been deployed, and (4) the Probe had begun to transmit. This was the first indication that the Huygens mission was going to be successful. The CSIRO Parkes Telescope also provided a direct detection of the Huygens carrier signal some two hours later and gave the first evidence that the Probe had landed and continued to transmit after landing. Two hours after the first detection, the Huygens carrier signal was also detected in the Mark 5 [Whitney, 2003] VLBI data recorded at the GBT. This was an important diagnostic of the overall performance of the VLBI part of the radio astronomy segment of the mission.

4.3. Express e-VLBI Demonstration in Support to the Huygens Mission

[41] Recent developments in information and radio astronomy technologies make it possible to transport large amounts of data from telescopes to processing centers thousands of kilometers apart via optical fiber lines. This kind of data transport enables a modification of the VLBI technique called e-VLBI [Szomoru et al., 2004]. Its major advantage lies in the elimination of recording media and shortening the delay between observations and obtaining results. The ultimate case of e-VLBI is real time VLBI. Over the last two decades, near-real-time transfer of narrow-band VLBI tracking data was exploited by NASA DSN for tracking planetary probes and other spacecraft with the transfer data rates of up to several Mbit/s [Thornton and Border, 2003].

[42] Since 2003, several observatories involved in Huygens VLBI tracking and JIVE were actively involved in wide-band e-VLBI research and development projects, including various demonstration tests with the transfer data rate of several hundreds Mbit/s. It was decided to apply the e-VLBI technique for a subset of Huygens VLBI tracking data, using high speed transmission and near real-time processing. Of the 17 radio telescopes listed in Table 1, two (the CSIRO Parkes Telescope and Mopra, both operated by the Australia Telescope National Facility, ATNF), were chosen for the Huygens e-VLBI demonstration. Huygens tracking at Parkes and Mopra was conducted using the LBA's hard-disk recording system, based on the Metsähovi VERSUSI input cards [Dodson et al., 2004]. Immediately after completion of the Huygens observations (late at night, local time in Australia), a charter plane flew

Table 3. Importance of Ground-Based Observations in Coordination With in Situ Planetary Missions

Topic	Examples	Selected References
Preparation of planetary missions	Target selection of cometary missions	
Scientific support during the mission	Study of Titan's atmosphere	<i>Griffith et al.</i> [2005] <i>Coustenis et al.</i> [2003, 2005] Sicardy et al. (submitted manuscript, 2006)
Relatively low cost of ground observations to space missions		
Large science returns of a joint effort	Huygens Deep impact	this special section <i>Meech et al.</i> [2005]
Extended temporal coverage	1. seasonal change in Titan's haze 1992–2002 from Hubble Space Telescope observations 2. study of stratospheric zonal winds	<i>Lorenz et al.</i> [2004] <i>Coustenis et al.</i> [2001] <i>Hirtzig et al.</i> [2005] <i>Luz et al.</i> [2006] <i>Kostiuk et al.</i> [2006]
Extended spatial or global coverage	zonal wind measurements with altitude coverage complementary to the Huygens DWE results	<i>Luz et al.</i> [2006] <i>Kostiuk et al.</i> [2006]
Different wavelength range	near-infrared observations above the Huygens DISR IR spectrometer limit	<i>Lellouch et al.</i> [2004] <i>Coustenis et al.</i> [2005] <i>Hirtzig et al.</i> [2006, submitted manuscript, 2006] Negrao et al. (submitted manuscript, 2006) <i>de Pater et al.</i> [2006] <i>Adámkovicš et al.</i> [2006]
Technique only possible from Earth.	1. VLBI radio tracking of Huygens probe and VEGA Venus Balloons to determine plane-of-sky probe motions (e.g., for wind determination) 2. Doppler radio tracking of Huygens and Galileo probes to provide Earth-relative probe velocity (e.g., for wind determination) 3. Doppler and range radio tracking of Mars Pathfinder and Viking landers to measure Mars rotational irregularities (e.g., for Mars interior structure and seasonal CO ₂ deposition) 4. radar evidence for liquid surfaces on Titan	<i>Lebreton et al.</i> [2005] <i>Preston et al.</i> [1986] <i>Sagdeev et al.</i> [1990] <i>Bird et al.</i> [2005] <i>Folkner et al.</i> [1997a] <i>Folkner et al.</i> [2006] <i>Folkner et al.</i> [1997b] <i>Campbell et al.</i> [2003]
Support in case of failure	Huygens radio astronomy segment following loss of Channel A	<i>Bird et al.</i> [2005] <i>Lebreton et al.</i> [2005] <i>Folkner et al.</i> [2006]
Necessary to achieve the science objectives of a given planetary mission	Deep Impact mission	<i>Meech et al.</i> [2005]
Information on aerothermodynamics during any atmospheric entry		<i>Lorenz et al.</i> [2006] <i>Magin et al.</i> [2006] <i>Caillault et al.</i> [2006]
Public outreach, amateur community	Deep Impact and Cassini-Huygens missions	

over the triangle Mopra – Parkes – Sydney to collect and deliver disks with the recorded data to the ATNF Headquarters in Epping. From there, two 15-min-long data segments recorded on one of the background celestial calibrator sources (a quasar) with a data rate of 512 Mbit/s, were transmitted via fiber optic cables over the Pacific, across North America and further on over the Atlantic to the JIVE

data processor in Dwingeloo, Netherlands. The total amount of about 900 Gbits was transmitted with the average data rate of about 300 Mbit/s. In the next step, the data were reformatted remotely at the Helsinki University of Technology from the “native” format for the ATNF telescope to the Mark 5 standard, suitable for correlation at JIVE. Another 0.5 hours were needed for JIVE staff to detect the interfer-

ometric “fringes” (response) on the baseline Parkes – Mopra. This detection was achieved about 13 hours after completion of the observations of the Huygens Probe at Parkes and Mopra.

[43] Interferometric fringes on the calibrator source obtained in the Huygens e-VLBI demonstration early in the morning of 15 January coupled with the detection of the Huygens channel A carrier signal at GBT and Parkes using both RSR and VLBI data acquisition during and soon after the mission on 14 January, provided a solid proof that the goal of the radio astronomy segment of the Huygens mission would be achieved.

[44] The “next morning” result of the express processing of data from the radio astronomy segment of the Huygens mission was an efficient verification of the correctness of the overall setup of the experiment, allowing the team to conclude, that the science goal of the experiment would be achieved in the course of full data processing. It also demonstrated a high potential of similar high data rate VLBI to support navigation of future planetary missions.

4.4. Attempt to Detect the Probe’s Entry

[45] Because of the STIS failure in August 2004, the HST observation was canceled. In addition, because of the cloudy weather in California and strong winds at the Mauna Kea summit, only the two observations with the Keck II and IRTF facilities were successful. However, no positive detection of the Probe entry was reported. No signal above $0.8 \mu\text{J}$ at the wavelength of $1.68 \mu\text{m}$ has been detected [*de Pater et al.*, 2006]. This does not permit to put significant constraints on the emission. *Lorenz et al.* [2006] provides all the details, and draws lessons learned for future observations of Probe’s entries.

[46] The modeling of the Huygens entry flux was the goal of an extensive set of studies, which took place in 2004 [*Walpot et al.*, 2005]. Two articles in this special section deal with such studies. *Magin et al.* [2006] describe a model that predicts the population of excited electronic states of the CN and N_2 molecules, in order to assess non-equilibrium radiation effects. *Caillault et al.* [2006] present radiative heat flux predictions for the Probe entry. The most intense emission originates from CN in the violet range. This study evaluates the role of the self-absorption by the plasma in reducing the total emission, and the effect of the chemical composition on the radiative heating.

5. Conclusion

[47] The Earth-based observations performed during or around the Huygens mission proved to be of fundamental importance: VLBI and Doppler measurements from the radio astronomy segment were essential in providing measurements of the Titan wind field during the Probe’s descent, which would have otherwise been lost because of the telecommunications problem. Observations with adaptive optics provided coverage of Titan’s hemisphere where Huygens landed. The zonal wind was measured at different altitudes by various methods, ideally complementing the Doppler Wind Experiment. Other scientific results were achieved concerning stratospheric temperatures, density and composition, cloud activity, haze distribution, surface albedo and composition. VLBI and Doppler measurements

provided (or will provide) useful information on the trajectory of the Huygens probe, which is very important for the data interpretation of the probe scientific data set. The real time detection of the probe carrier signal during descent indicated that the probe survived the entry and started transmitting data. No positive detection of the probe entry was reported. However, lessons learned are published in this special section. Comprehensive studies on heat fluxes and heat loads were carried out and will be very valuable for future planetary probe entries. Finally, these observations represented a “down-to-Earth” aspect of the mission of prime interest to the media and general public.

[48] The recent Deep Impact event is another example of coordinated ground-based observations [*Meech et al.*, 2005]. In this case seven Earth-orbiting spacecraft, a large number of telescopes and the ESA comet chaser Rosetta were observing comet 9P/Tempel 1 when hit by the impactor.

[49] The utility of ground-based (or Earth-based) observations is summarized in Table 3. Future opportunities for coordinated, supporting and complementary observations to space missions include: Cassini in the Saturnian system (end of nominal mission: mid 2008), Mars Express at Mars (mission extended until October 2007), Venus Express at Venus (orbit insertion on 11 April 2006, end of nominal mission in October 2007), Chandrayaan-1, Selene and Chang’e-1 around the Moon (2007–2009), Messenger at Venus (flyby) and Mercury, Bepi-Colombo at Mercury, Rosetta (Mars flyby in February 2007, asteroid flybys in 2008 and 2010, at comet 67P/Churyumov-Gerasimenko 2014–2015), New Horizons at Jupiter in 2007 and at Pluto in 2015.

[50] The results presented in this special section represent the achievements one year after Huygens. It is clear that a significant part of the data is still being analyzed, and we expect many more scientific results in the coming months and years.

[51] **Acknowledgments.** The decision to support and coordinate a series of optical ground-based observations was taken at the time of the Huygens Science Working Team in October 2003 in Graz. We thank all participants, especially Athena Coustenis and Dennis Matson, for their support. We thank the observatory directors and telescope allocation panels for their endorsement of all these observations. We thank the European funded network EUROPLANET for its support. This research was carried out in part at the Jet Propulsion Laboratory, California Institute of Technology, under contract with NASA. We appreciate the support provided by the National Radio Astronomy Observatory (NRAO) and the Australia Telescope National Facility (ATNF). NRAO is operated by Associated Universities, Inc., under a cooperative agreement with the NSF. The ATNF, managed by the Commonwealth Scientific and Industrial Research Organization (CSIRO), The Joint Institute for VLBI in Europe, is funded by the national research councils, national facilities and institutes of Netherlands (NWO), the United Kingdom (PPARC), Italy (INAF), Sweden (Onsala Space Observatory, National Facility), Spain (IGN), Germany (MPIfR), and China (National Astronomical Observatories, CAS). The Huygens e-VLBI demonstration would have been impossible without the efforts of the networking community, who on very short notice provisioned a dedicated light path between Australia and JIVE. We thank George McLaughlin, Steve Maddocks, Mark Prior, and Alan Cowie (AARNet), Shaun Amy (CSIRO), Craig Russell (CeNTIE), Hervé Guy and Damiir Pobric (Canarie), Bill Mar (Pacific Northwest GigaPop), Geoff Lakeman (University of Washington), Caroline Carver (MANLAN), and Dennis Paus (SURFnet). Part of this work was funded through grants AST-0205893 from the National Science Foundation and NNG05GH63G from NASA to the Univ. of California, Berkeley. David Luz acknowledges financial support from Fundação para a Ciência e a Tecnologia, Portugal (fellowship PRAXIS XXI/BPD/3630/2000 and project POCI/CTE-AST/57655/2004). Alberto Negrão is supported by the FCT Ph.D. scholarship SFRH/BD/

8006/2002. HIPWAC measurements were supported by the NASA Planetary Astronomy Program. Olivier Witasse thanks Sushil Atreya for useful suggestions.

References

- Ádámkóvics, M., I. de Pater, H. G. Roe, S. G. Gibbard, and C. A. Griffith (2004), Spatially-resolved spectroscopy at 1.6 μm of Titan's atmosphere and surface, *Geophys. Res. Lett.*, **31**, L17S05, doi:10.1029/2004GL019929.
- Ádámkóvics, M., I. de Pater, M. Hartung, F. Eisenhauer, R. Genzel, and A. Griffith (2006), Titan's bright spots: Multiband spectroscopic measurement of surface diversity and hazes, *J. Geophys. Res.*, **111**, E07S06, doi:10.1029/2005JE002610.
- Barnes, J. W., et al. (2005), A 5-Micron-bright spot on Titan: Evidence for surface diversity, *Science*, **310**, 92–95.
- Bird, M. K., et al. (2005), The vertical profile of winds on Titan, *Nature*, **438**, 800–802.
- Caillault, L., et al. (2006), Radiative heating predictions for Huygens entry, *J. Geophys. Res.*, doi:10.1029/2005JE002627, in press.
- Campbell, D., et al. (2003), Radar evidence for liquid surfaces on Titan, *Science*, **302**(5644), 431–434.
- Counselman, C., S. Gourevitch, R. King, G. Pettengill, I. Shapiro, R. Miller, J. Smith, R. Prinn, R. Ramos, and P. Leibrich (1979), Wind velocities on Venus: Vector determination by radio interferometry, *Science*, **230**, 805–806.
- Coustenis, A., E. Gendron, O. Lai, J.-P. Veran, J. Woillez, M. Combes, L. Vapillon, Th. Fusco, L. Mugnier, and P. Rannou (2001), Images of Titan at 1.3 and 1.6 microns with adaptive optics at the CFHT, *Icarus*, **154**, 501–515.
- Coustenis, A., A. Salama, B. Schulz, S. Ott, E. Lellouch, T. H. Encrenaz, D. Gautier, and H. Feuchtgruber (2003), Titan's atmosphere from ISO mid-infrared spectroscopy, *Icarus*, **161**(2), 383–403.
- Coustenis, A., M. Hirtzig, E. Gendron, P. Drossart, O. Lai, M. Combes, and A. Negro (2005), Maps of Titan's surface from 1 to 2.5 micron, *Icarus*, **177**, 89–105.
- de Pater, I., M. Ádámkóvics, A. H. Bouchez, M. E. Brown, S. G. Gibbard, F. Marchis, H. G. Roe, E. L. Schaller, and E. Young (2006), Titan imagery with Keck adaptive optics during and after probe entry, *J. Geophys. Res.*, **111**, E07S05, doi:10.1029/2005JE002620.
- Dodson, R., S. Tingay, C. West, C. Phillips, A. Tzioumis, J. Ritakari, and F. Briggs (2004), The Australian experience with the PC-EVN recorder, in *Proceedings of the 7th European VLBI Symposium*, edited by R. Bachiller et al., p. 253, Observ. Astron. Nacl., Toledo, Spain.
- Flasar, F. M., et al. (2005), Titan's atmospheric temperatures, winds, and composition, *Science*, **308**, 975–978.
- Folkner, W. M., et al. (1997a), Earth-based radio tracking of the Galileo probe for Jupiter wind estimation, *Science*, **275**, 644–646.
- Folkner, W. M., et al. (1997b), Interior structure and seasonal mass redistribution of Mars from radio tracking of Mars Pathfinder, *Science*, **278**, 1749–1752.
- Folkner, W. M., et al. (2006), Winds on Titan from ground-based tracking of the Huygens probe, *J. Geophys. Res.*, **111**, E07S02, doi:10.1029/2005JE002649.
- Fulchignoni, M., et al. (2005), In situ measurements of the physical characteristics of Titan's atmosphere, *Nature*, **438**, 785–791.
- Gibbard, S. G., I. de Pater, B. A. Macintosh, H. G. Roe, C. E. Max, E. F. Young, and C. P. McKay (2004), Titan's 2 μm surface albedo and haze optical depth in 1996–2004, *Geophys. Res. Lett.*, **31**, L17S02, doi:10.1029/2004GL019803.
- Griffith, C., et al. (2005), Observations of Titan's mesosphere, *Astrophys. J.*, **629**(1), L57–L60.
- Hartung, M., T. M. Herbst, C. Dumas, T. Owen, and A. Coustenis (2006), Limits to the abundance of surface CO₂ ice on Titan, *J. Geophys. Res.*, **111**, E07S09, doi:10.1029/2005JE002642.
- Hirtzig, M., A. Coustenis, O. Lai, E. Emsellem, A. Pecontal-Rousset, P. Rannou, A. Negro, and B. Schmitt (2005), Near-infrared study of Titan's resolved disk in spectro-imaging with CFHT/OASIS, *Planet. Space Sci.*, **53**, 535–556.
- Hirtzig, M., A. Coustenis, E. Gendron, P. Drossart, A. Negro, M. Combes, O. Lai, P. Rannou, S. Lebonnois, and D. Luz (2006), Monitoring atmospheric phenomena on Titan, *Astron. Astrophys.*, in press.
- Israel, G., et al. (2005), Complex organic matter in Titan's atmospheric aerosols from in situ pyrolysis and analysis, *Nature*, **438**, 796–799.
- King, R. W., C. C. Counselman III, and I. I. Shapiro (1976), Lunar dynamics and selenodesy: Results from analysis of VLBI and laser data, *J. Geophys. Res.*, **81**, 6251–6256.
- Kostiuk, T., K. Fast, T. A. Livengood, T. Hewagama, J. Goldstein, F. Espenak, and D. Buhl (2001), Direct measurement of winds on Titan, *Geophys. Res. Lett.*, **28**, 2361–2364.
- Kostiuk, T., T. A. Livengood, T. Hewagama, G. Sonnabend, K. E. Fast, K. Murakawa, A. T. Tokunaga, J. Annen, D. Buhl, and F. Schmitt (2005), Titan's stratospheric zonal wind, temperature, and ethane abundance a year prior to Huygens insertion, *Geophys. Res. Lett.*, **32**, L22205, doi:10.1029/2005GL023897.
- Kostiuk, T., et al. (2006), Stratospheric global winds on Titan at the time of Huygens descent, *J. Geophys. Res.*, doi:10.1029/2005JE002630, in press.
- Lebreton, J.-P., et al. (2005), An overview of the descent and landing of the Huygens probe on Titan, *Nature*, **438**, 758–764.
- Lellouch, E., B. Schmitt, A. Coustenis, and J.-G. Cuby (2004), Titan's 5-micron lightcurve, *Icarus*, **168**, 209–214.
- Lorenz, R. D., P. H. Smith, and M. T. Lemmon (2004), Seasonal change in Titan's haze 1992–2002 from Hubble Space Telescope observations, *Geophys. Res. Lett.*, **31**, L10702, doi:10.1029/2004GL019864.
- Lorenz, R. D., et al. (2006), Huygens entry emission: Observation campaign, results, and lessons learned, *J. Geophys. Res.*, **111**, E07S11, doi:10.1029/2005JE002603.
- Luz, D., et al. (2006), Characterization of zonal winds in the stratosphere of Titan with UVES: Ii: Observations coordinated with the Huygens entry, *J. Geophys. Res.*, doi:10.1029/2005JE002617, in press.
- Magin, T. E., L. Caillault, A. Bourdon, and C. O. Laux (2006), Nonequilibrium radiative heat flux modeling for the Huygens entry probe, *J. Geophys. Res.*, **111**, E07S12, doi:10.1029/2005JE002616.
- Meech, K. J., et al. (2005), Deep impact: Observations from a worldwide Earth-based campaign, *Science*, **310**, 265–269.
- Moreno, R., A. Marten, and T. Hidayat (2005), Interferometric measurements of zonal winds on Titan, *Astron. Astrophys.*, **437**, 319–328.
- Niemann, H. B., et al. (2005), The abundances of constituents of Titan's atmosphere from the GCMS instrument on the Huygens probe, *Nature*, **438**, 779–784.
- Pogrebenko, S. V., L. I. Gurvits, R. M. Campbell, I. M. Avrukh, J.-P. Lebreton, and C. G. M. van't Klooster (2004), VLBI tracking of the Huygens probe in the atmosphere of Titan, in *Proceedings of the International Workshop "Planetary Probe Atmospheric Entry and Descent Trajectory Analysis and Science"*, Lisbon, Portugal, 5–9 October 2003, *Eur. Space Agency Spec. Publ.*, **ESA-SP 544**, 197–204.
- Preston, R. A., et al. (1986), Determination of Venus winds by ground-based radio tracking of the VEGA balloons, *Science*, **231**, 1414–1416.
- Sagdeev, R. Z., et al. (1990), Measurements of the dynamics of air mass motion in the Venus atmosphere with balloon probes—VEGA Project, *Sov. Astron. Lett.*, **16**, 357.
- Sagdeyev, R. Z., et al. (1992), Differential VLBI measurements of the Venus atmosphere dynamics by balloons—VEGA Project, *Astron. Astrophys.*, **254**, 387.
- Schaller, E. L., M. E. Brown, H. G. Roe, A. H. Bouchez, and C. A. Trujillo (2005), Cloud activity on Titan during the Cassini mission, *Proc. Lunar Planet. Sci. Conf. 36th*, abstract 1989.
- Schaller, E. L., M. E. Brown, H. G. Roe, and A. H. Bouchez (2006), A large cloud outburst at Titan's south pole, *Icarus*, **182**, 224–229.
- Slade, M. A., R. A. Preston, A. W. Harris, L. J. Skjerve, and D. J. Spitzmesser (1977), ALSEP-Quasar Differential VLBI, *Moon*, **17**, 133.
- Szomoru, A., A. Biggs, M. Garrett, H. J. van Langevelde, F. Olon, Z. Paragi, S. Parsley, S. Pogrebenko, and C. Reynolds (2004), From truck to optical fibre: The coming-of-age of eVLBI, in *Proceedings of the 7th European VLBI Symposium*, edited by R. Bachiller et al., p. 257, Observ. Astron. Nacl., Toledo, Spain.
- Thornton, C. L., and J. S. Border (2003), *Radiometric Tracking Techniques for Deep-Space Navigation*, John Wiley, Hoboken, N. J.
- Tomasko, M. G., et al. (2005), Rain, winds and haze during the Huygens probe's descent to Titan's surface, *Nature*, **438**, 765–778.
- Walpot, L., L. Caillault, C. O. Laux, R. Molina, and T. Blancaquert (2005), Huygens entry heat flux prediction, paper presented at 3rd International Planetary Probe Workshop (IPPW-3), Am. Inst. of Aeronaut. and Astronaut., Attica, Greece, July.
- Whitney, A. R. (2003), Mark 5 disk-based Gbps VLBI data system, in *New Technology in VLBI*, edited by Y. C. Minh, *ASP Conf. Ser.* **306**, p. 123, Astron. Soc. of the Pac., San Francisco, Calif.
- Yelle, R. V., D. Strobel, E. Lellouch, and D. Gautier (1997), Engineering models for Titan's atmosphere, in *Huygens: Science, Payload and Mission*, edited by J.-P. Lebreton, *Eur. Space Agency Spec. Publ.*, **ESA-SP 1177**, 243–256.
- Zarnecki, J. C., et al. (2005), A soft solid surface on Titan as revealed by the Huygens Surface Science Package, *Nature*, **438**, 792.

M. Ádámkóvics and I. de Pater, Department of Astronomy, University of California, 601 Campbell Hall, Berkeley, CA 94720, USA.

S. W. Asmar, B. J. Buratti, W. M. Folkner, and R. A. Preston, Jet Propulsion Laboratory, California Institute of Technology, Pasadena, CA 91109, USA.

I. M. Avruch, H. E. Bignall, R. M. Campbell, M. A. Garrett, L. I. Gurvits, S. M. Parsley, S. V. Pogrebenko, C. Reynolds, A. Szomoru, and H. J. van Langevelde, Joint Institute for VLBI in Europe, P.O. Box 2, 7990 AA, Dwingeloo, Netherlands.

M. K. Bird and R. Dutta-Roy, Radioastronomisches Institut, Universität Bonn, Auf dem Hügel 71, D-53125 Bonn, Germany.

T. Blancquaert and C. G. M. van't Klooster, ESA, ESTEC, TEC Directorate, Noordwijk, 2200 AG, Netherlands.

A. H. Bouchez, Caltech Optical Observatories, California Institute of Technology, MS 150-21, Pasadena, CA 91125, USA.

A. Bourdon, L. Caillault, C. Laux, and T. Magin, Laboratoire EM2C, Ecole Centrale Paris, CNRS-UPR288, Grande Voie des Vignes, F-92295 Châtenay-Malabry, France.

W. Briskin and J. D. Romney, National Radio Astronomy Observatory, P.O. Box 0, 1003 Lopezville Road, Socorro, NM 87801, USA.

M. Brown, H. Roe, and E. Schaller, Division of Geological and Planetary Sciences, California Institute of Technology, MS 150-21, Pasadena, CA 91125, USA.

A. Coustenis, E. Gendron, M. Hirtzig, D. Luz, A. Negro, and B. Sicardy, LESIA, Observatoire Paris-Meudon, F-92195 Meudon Cedex, France.

R. G. Dodson, Observatorio Astronómico Nacional, Apartado 112, 28803 Alcalá de Henares, Spain.

F. Ghigo and G. Langston, National Radio Astronomy Observatory, P.O. Box 2, Rt. 28/92, Green Bank, WV 24944, USA.

M. Hartung, European Southern Observatory, Alonso de Cordova 3107, Santiago 19, Chile.

T. Kostiuik, NASA Goddard Space Flight Center, Greenbelt, MD 20771, USA.

J.-P. Lebreton and O. Witasse, Research and Scientific Support Department, ESA, ESTEC, Noordwijk, 2200 AG, Netherlands. (owitasse@rssd.esa.int)

T. A. Livengood, National Center for Earth and Space Science Education, Washington, DC 20036, USA.

R. D. Lorenz, Lunar and Planetary Laboratory, University of Arizona, Tucson, AZ 85721, USA.

A. Mujunen and J. Ritakari, Metsähovi Radio Observatory, Helsinki University of Technology, Metsähovintie 114, FIN-02540 Kylmälä, Finland.

C. J. Phillips, J. E. Reynolds, R. J. Sault, and A. K. Tzioumis, Australia Telescope National Facility, CSIRO, P.O. Box 76, Epping, NSW 1710, Australia.

S. J. Tingay, Swinburne University of Technology, P.O. Box 218, Hawthorn 3122, Australia.

C. A. Trujillo, Gemini Observatory, Hilo, HI 96720, USA.